

Supplementary Information

Effective separation of surfactant-stabilized crude oil-in-water emulsions by waste brick powders-coated membrane under corrosive conditions

Guogui Shi^a, Yongqian Shen^b, Peng Mu^a, Qingtao Wang^a, Yaoxia Yang^a, Siyi Ma^a, Jian Li^{*,a}

^a Gansu International Scientific and Technological Cooperation Base of Water-retention Chemical Functional Materials, College of Chemistry and Chemical Engineering, Northwest Normal University, Lanzhou 730070, P. R. China. E-mail: jianli83@126.com, Tel: +86 931 7971533

^b State Key Laboratory of Advanced Processing and Recycling of Non-ferrous Metals, School of Materials Science & Engineering, Lanzhou University of Technology, Lanzhou 730050, P. R. China. E-mail: syqch@163.com

Supplementary figure

Figure S1. FE-SEM images of (a) the original and (b) acidified WBP at low and high magnifications, respectively.

Figure S2. Relationship between the volume of the suspension and the average pore size and separation performance of the membrane.

Figure S3. (a) EDS mapping image and (b) EDS analysis of the WBP-coated membrane, respectively.

Figure S4. FT-IR spectra of the sodium alginate.

Figure S5. Photographs of (a) WBP-coated membrane and (b) original PVDF membrane contaminated by crude oil, respectively.

Figure S6. (a) Photograph of the WBP-coated membrane. (b) The vacuum-driven filtration system. (c) Photograph after separation of crude oil-in-water emulsions.

Figure S7. Optical microscope images, digital images and droplet size distribution of different emulsions and filtrates: (a) kerosene-in-water emulsions, (b) n-hexane-in-water emulsions and (c) petroleum ether-in-water emulsions, respectively.

Figure S8. Changes in permeating flux of crude oil-in-water emulsions over time.

Figure S9. Optical images and FE-SEM of waste brick powders-coated membrane after immersing for different time.

Figure S10. Optical microscope images, digital images and droplet size distribution of different emulsions and filtrates: (a) crude oil-in-HCl emulsions and (b) crude oil-in-NaCl emulsions, respectively.

Figure S11. (a) Permeating flux, (b) separation efficiency and oil contents of the

WBP-coated membrane for the kerosene-in-water emulsions under corrosive environments, respectively.

Figure S12. Optical microscope images, digital images and droplet size distribution of different emulsions and filtrates: (a) kerosene-in-HCl emulsions, (b) kerosene-in-NaOH emulsions and (c) kerosene-in-NaCl emulsions, respectively.

Table S1. The properties of the PVDF.

Movie S1. The movie of WBP-coated membrane separating crude oil-in-water emulsions membrane.

Moive S2. The movie of pure PVDF membrane separating crude oil-in-water emulsions.

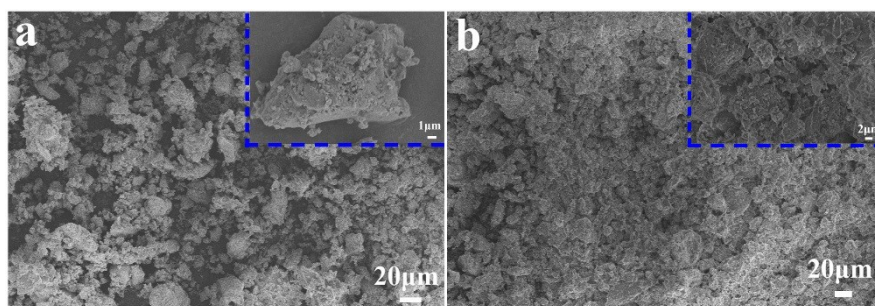


Figure S1. FE-SEM images of (a) the original and (b) acidified WBP at low and high magnifications, respectively.

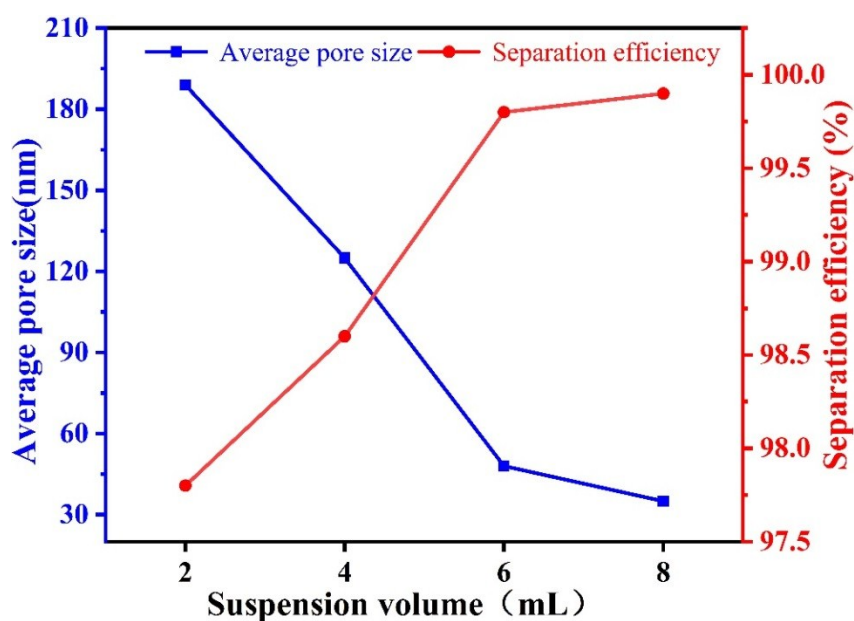


Figure S2. Relationship between the volume of the suspension and the average pore size and separation performance of the membrane.

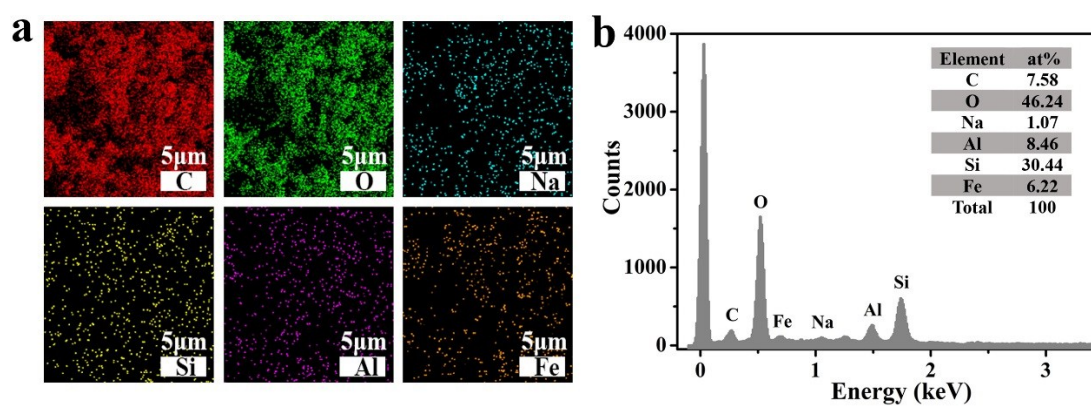


Figure S3. (a) EDS mapping image and (b) EDS analysis of the WBP-coated membrane, respectively.

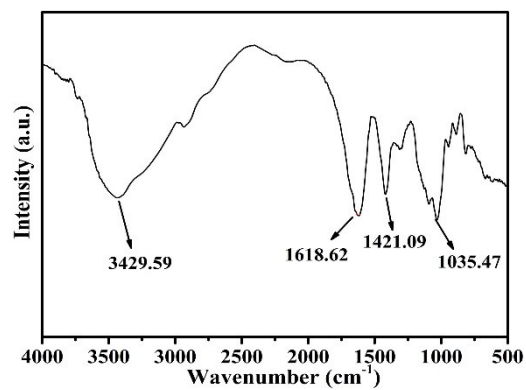


Figure S4. FT-IR spectra of the sodium alginate.

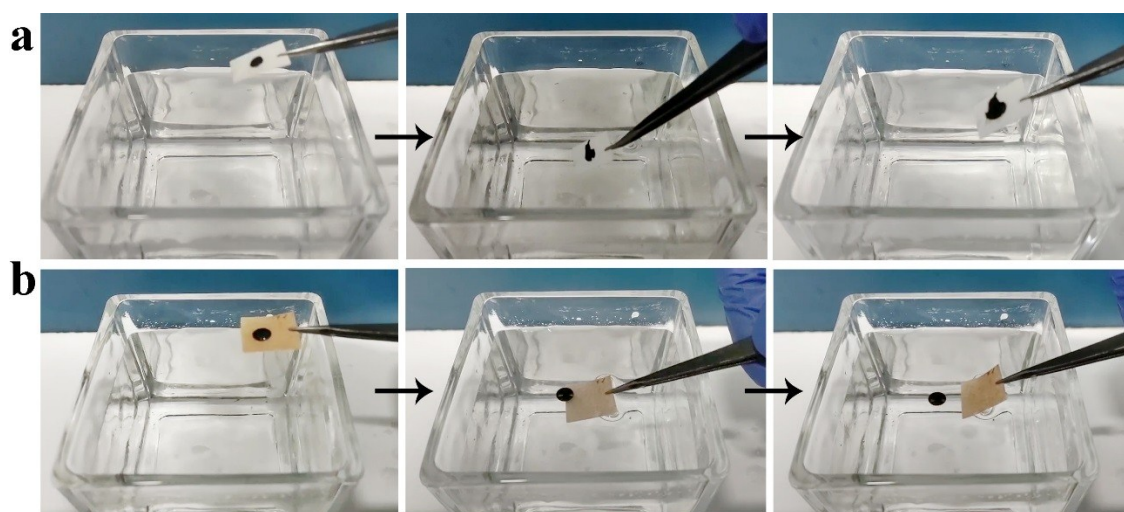


Figure S5. Photographs of (a) WBP-coated membrane and (b) original PVDF membrane contaminated by crude oil, respectively.

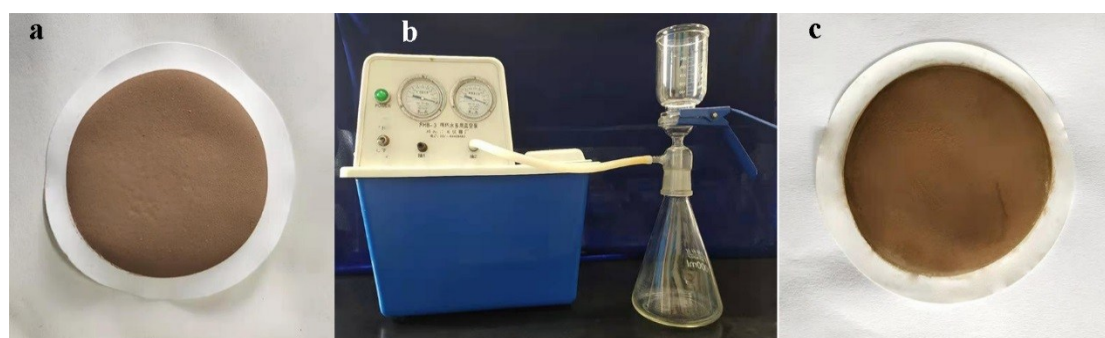


Figure S6. (a) Photograph of the WBP-coated membrane. (b) The vacuum-driven filtration system. (c) Photograph after separation of crude oil-in-water emulsions.

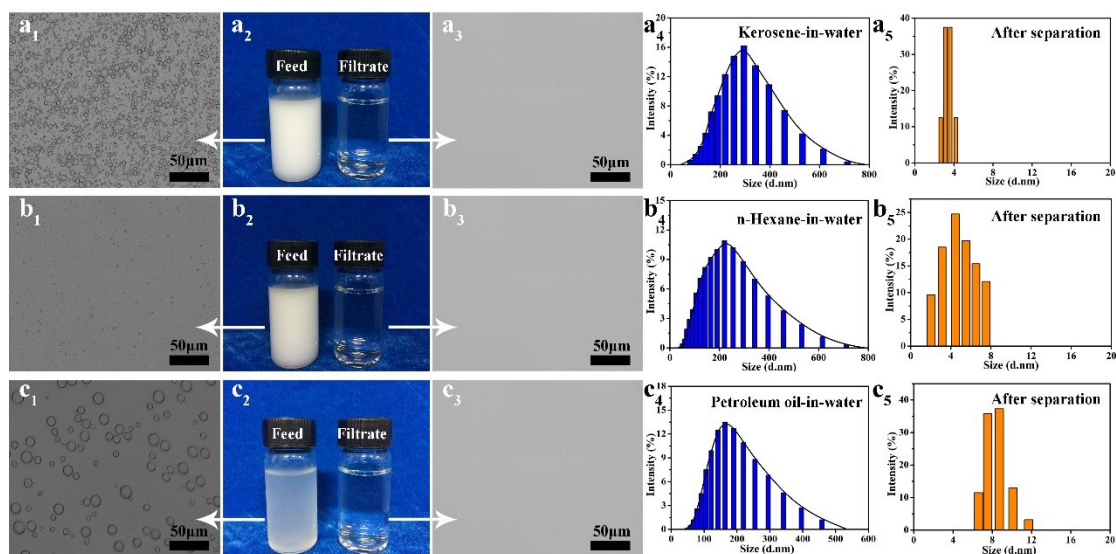


Figure S7. Optical microscope images, digital images and droplet size distribution of different emulsions and filtrates: (a) kerosene-in-water emulsions, (b) n-hexane-in-water emulsions and (c) petroleum ether-in-water emulsions, respectively.

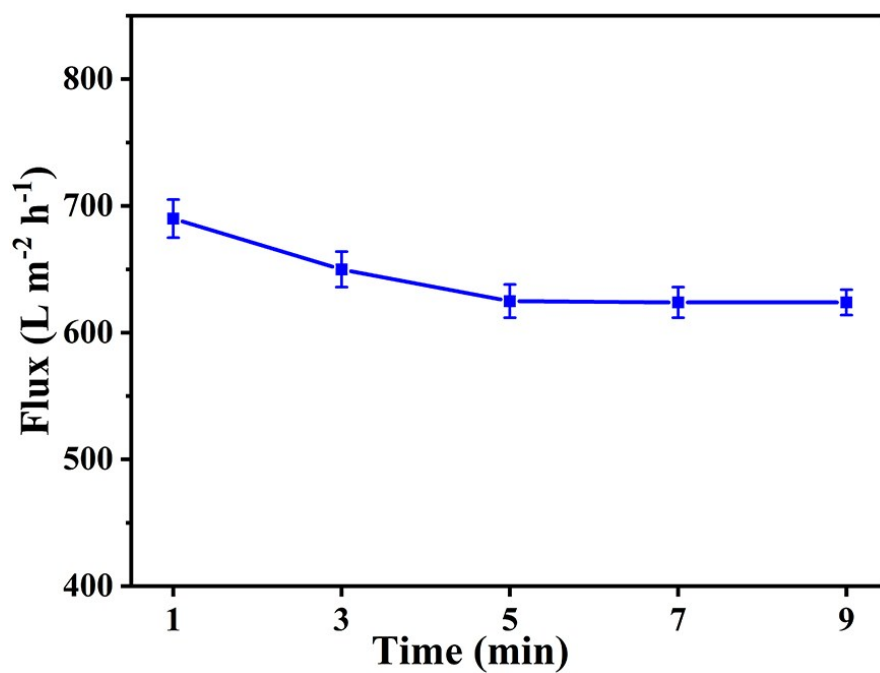


Figure S8. Changes in permeating flux of crude oil-in-water emulsions over time.

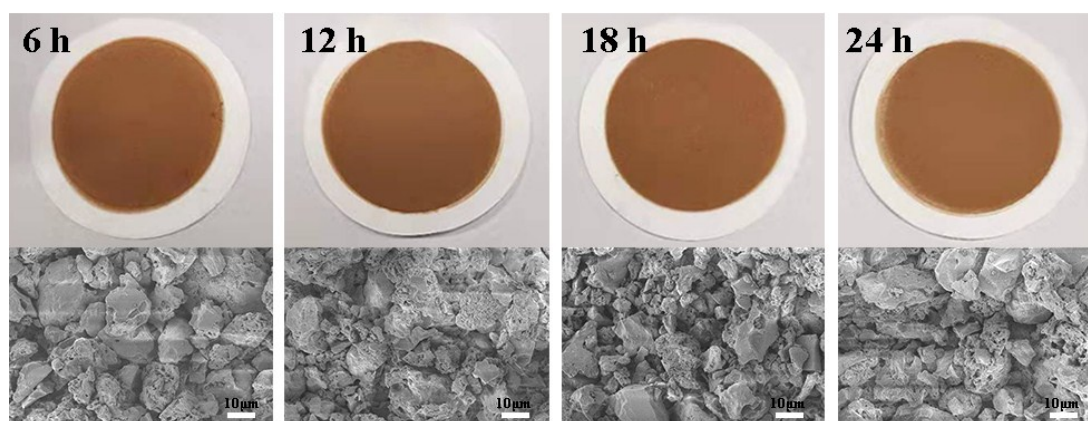


Figure S9. Optical images and FE-SEM of waste brick powders-coated membrane after immersing for different time.

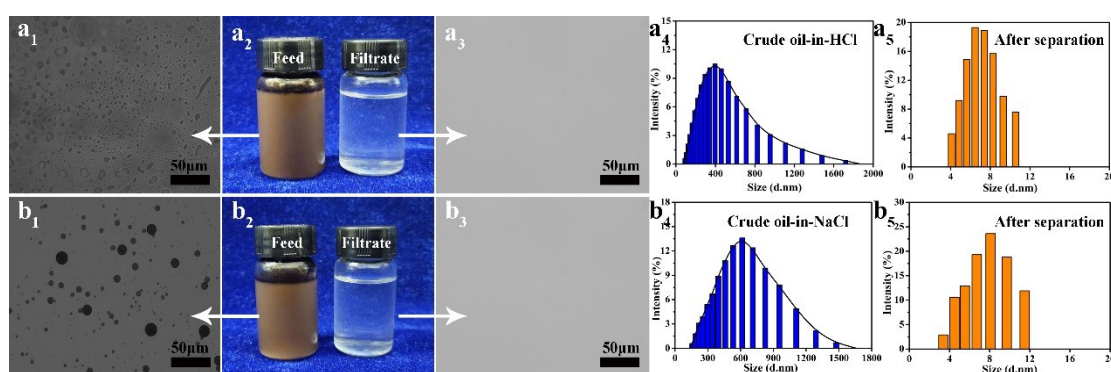


Figure S10. Optical microscope images, digital images and droplet size distribution of different emulsions and filtrates: (a) crude oil-in-HCl emulsions and (b) crude oil-in-NaCl emulsions, respectively.

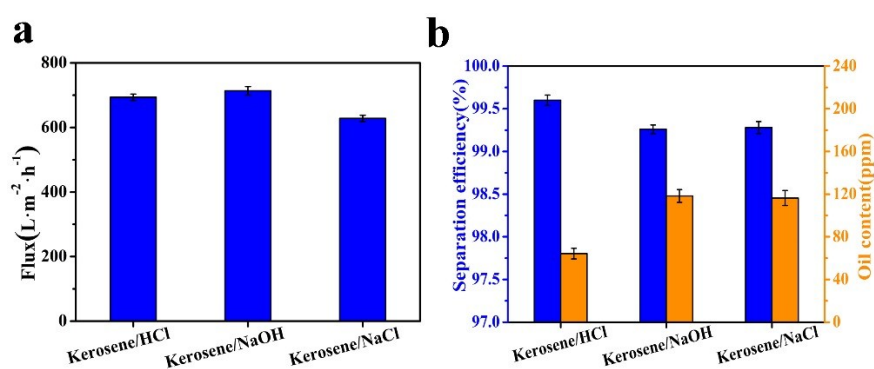


Figure S11. (a) Permeating flux, (b) separation efficiency and oil contents of the WBP-coated membrane for the kerosene-in-water emulsions under corrosive environments, respectively.

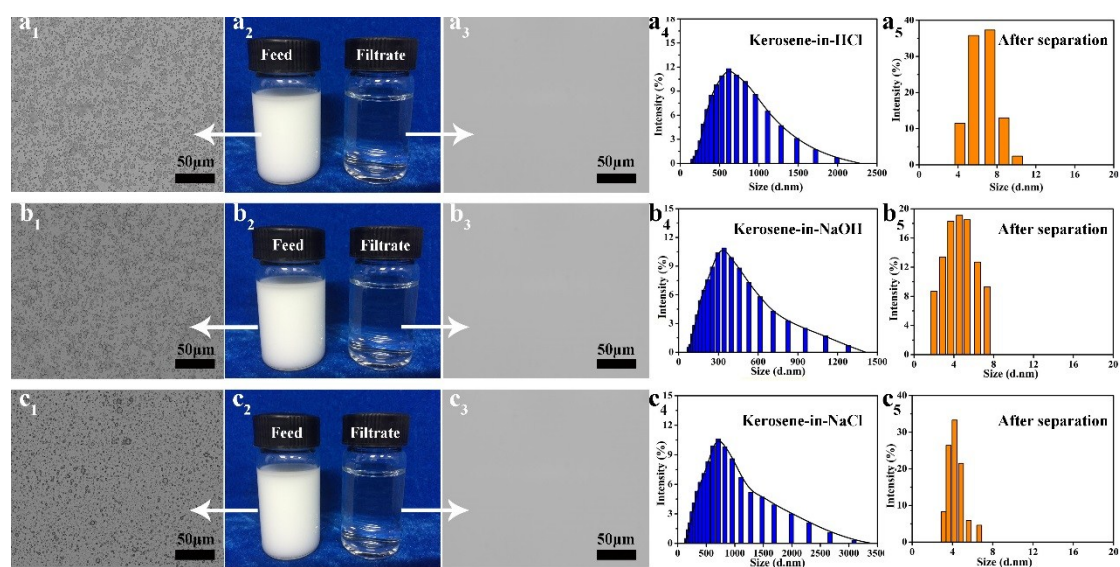


Figure S12. Optical microscope images, digital images and droplet size distribution of different emulsions and filtrates: (a) kerosene-in-HCl emulsions, (b) kerosene-in-NaOH emulsions and (c) kerosene-in-NaCl emulsions, respectively.

Table S1. The properties of the PVDF.

Type	Thickness (μm)	Diameter (mm)	Pore diameter (μm)	Porosity (%)
F-type	150	50	0.45	90%